Respiratory Therapy Theses   Department of Respiratory Therapy

5-10-2021

Does Increasing Flow to a High-flow Nasal Cannula Affect Mean Airway Pressure in a Pediatric In Vitro Model?

James Liu

Follow this and additional works at: https://scholarworks.gsu.edu/rt_theses

DOES INCREASING FLOW TO A HIGH-FLOW NASAL CANNULA (HFNC)
AFFECT MEAN AIRWAY PRESSURE (MAP) IN A PEDIATRIC IN VITRO MODEL?

By

James Chen-Chiau Liu

A Thesis

Presented in Partial Fulfillment of the Requirements for the

Degree of

Master gf Science

in

Health Sciences

in

the Department of Respiratory Therapy

Under The Supervision of Dr. Douglas S. Gardenhire

in

Byrdine F. Lewis College of Nursing And Health Professions

Georgia State University

Atlanta, Georgia
2021

ACCEPTANCE

This thesis, DOES INCREASING FLOW TO A HIGH-FLOW NASAL CANNULA AFFECT MEAN AIRWAY PRESSURE IN A PEDIATRIC IN VITRO MODEL?, by James Liu, was prepared under the direction of the candidate's thesis committee. It is accepted by the committee members in partial fulfillment of the requirements for the degree of Master of Science in Respiratory Therapy in the Byrdine F. Lewis College of Nursing and Health Professions, Georgia State University.

Approved by:

_____
Douglas S. Gardenhire, EdD, RRT, RRT-NPS, FAARC
Committee Chair

_____
Robert B. Murray, MS, RRT
Committee Member

_____
Kyle J. Brandenberger, PhD
Committee Member

_____
Date

AUTHOR'S STATEMENT

In presenting this thesis as a partial fulfillment of the requirements for the advanced degree from Georgia State University, I agree that the library of Georgia State University shall make it available for inspection and circulation in accordance to its regulations governing materials of this type. I agree that permission to quote, to copy from, or to publish this thesis may be granted by the professor under which direction it was written, or by me. Such quoting, copying, or publishing must be solely for scholarly purposes and will not involve potential financial gain. It is understood that any copying from or publication of this thesis which involves potential financial gain will not be allowed without my written permission.

_____

James Chen-Chiau Liu

NOTICE TO BORROWERS

All theses deposited in the Georgia State University library must be used in accordance with the

stipulations prescribed by the author in the preceding statement.

The author of this thesis is:

James Chen-Chiau Liu

12303 Jefferson Square Court

Decatur, GA 30030

JamesCL90@gmail.com

The director of this thesis is:

Douglas S. Gardenhire, EdD, RRT, RRT-NPS, FAARC

Lewis College of Nursing and Health Professionals

Georgia State University

Atlanta, Georgia 30303-3083

Users of this thesis who are not regularly enrolled as students at Georgia State University are
required to attest acceptance of the preceding stipulation by signing below. Libraries borrowing
this thesis for the use of their own patrons are required to see that each user records here the
information requested.

NAME OF USER	ADDRESS	DATE	TYPF OF USE (EXAMINATION ONLY OR COPYING)

DEDICATION

I would like to thank those who have supported me in reaching this point in my education as well as guide me through this entire process. To my part-time mentor, full-time fiancé, and forever adventure buddy, I cannot express the depth of my appreciation for putting up with me. To my family who has constantly pushed me towards a brighter future, also thank you. I would also like to spread some thanks to my professors for enduring my relentless curiosity for the duration of the program and thesis preparation.

ACKNOWLEDGEMENTS

Sincere thanks goes out to Dr. Douglas Gardenhire, Professor Brent Murray, and Dr. Kyle Brandenberger for their time and commitment to completing this thesis. This would have been impossible without all of your help.

CURRICULUM VITAE

James Chen-Chiau Liu
12303 JEFFERSON SQUARE COURT
DECATUR, GA 30030

EDUCATION: M.S. 2021 GEORGIA STATE UNIVERSITY
HEALTH SCIENCE

B.S. 2017 GEORGIA STATE UNIVERSITY
HEALTH INFORMATICS

PROFESSIONAL EXPERIENCE:

MAY-JUNE 2020   GRADUATE TEACHING ASSISTANT
DIVISION OF RESPIRATORY THERAPY
GEORGIA STATE UNIVERSITY, ATLANTA, GA

SEPT-DEC 2019.   GRADUATE ANATOMY & PHYSIOLOGY TUTOR
DIVISION OF BIOLOGY
GEORGIA STATE UNIVERSITY, ATLANTA, GA

DOES INCREASING FLOW TO A HIGH-FLOW NASAL CANNULA (HFNC)
AFFECT MEAN AIRWAY PRESSURE (MAP) IN A PEDIATRIC IN VITRO MODEL?

By

James Chen-Chiau Liu

(Under the Direction of Dr. Douglas S. Gardenhire)

ABSTRACT

Introduction: High flow nasal cannulas (HFNC) are an oxygen supply device that has become increasingly popular. This high flow therapy was initially utilized in the neonatal populations for treatment of conditions such as bronchiolitis and respiratory distress. The mechanism of treatment behind HFNC in these conditions relies upon the large amount of flow which produces continuous positive airway pressure (CPAP) against the airways. This pressure maintains the structural patency of the airway, allowing for continuous flow during inspiration and expiration. The small amount of CPAP generated by the HFNC assists in oxygenation and gas exchange by expanding the size of alveoli at end expiration and generating a greater surface area for diffusion across the alveolar capillary membrane. The purpose of this study was to determine if greater flows generated from the HFNC to a pediatric in vitro model would affect the mean airway pressure (MAP). **Method:** A pediatric in vitro model was utilized to simulate two spontaneous breathing patterns with the use of a Dual Adult Test and Training Lung (TTL) connected to a Hamilton-G5 ventilator. Positive pressure ventilation delivered to one side A of the Dual Adult TTL simulated a spontaneously breathing negative pressure model on the other side B of the Dual Adult TTL. The two sides of the Dual Adult TTL were connected via a wooden board and clamped to cause simultaneous movement of both lungs. HFNC delivered flow to side B through a fabricated airway. A pressure sensor placed between the MIL TTL and the fabricated airway and connected to an auxiliary pressure monitoring port on the Hamilton-G5 ventilator. Three different HFNC were used and tested at two various flows (10, 15, and 20 liters per minute (L/min)) and two different respiratory patterns (labored and unlabored). No other parameters were changed. **Data Analysis:** two-way analysis of variance (ANOVA), descriptive statistics, and post hoc Bonferroni were used for this study. SPSS 26.0 for Windows was used for all data analysis in this study **Results:** The average MAP produced by all three HFNC were increased at all flow rates. Greater flow rates up to 20 L/min created a greater amount of MAP, an average of 2.34 cm H_2O and 2.49 for unlabored and labored breathing pattern respectively at 20 L/min. The Hudson HFNC generated the greatest MAP of all three HFNC (3.81 cm H_2O at 20 L/min, labored breathing pattern). Based on ANOVA analysis, increased flows through all devices were statistically significant based on a *p* value of 0.05. **Conclusions:** A significant difference in MAP was found between flow rates for all devices and simulated breathing patterns, devices for all flow rates and simulated breathing patterns, and both simulated breathing patterns for all devices and flow rates.

TABLE OF CONTENTS

CHAPTER I

INTRODUCTION

The high flow nasal cannula (HFNC) is an increasingly popular piece of equipment that provides a moderate-to-high amount of flow to patients through the nasal passage (Lodeserto, 2018). The benefits of high flow therapy are twofold: to provide a small degree of pressure to the airway and parenchyma and to washout physiological dead space from the airway (Nishimura, 2016; Spoletini et al., 2015; Spicuzza & Schisano, 2020) . The dead space washout helps a patient in multiple ways. First, we must present the conditions most affected by dead space, the increase in carbon dioxide (CO_2) within the body known as hypercapnia, and the decrease in oxygen within the body known as hypoxia (Frat et al., 2015). Hypercapnia is an elevated amount of carbon dioxide (CO_2) in a person's body. CO_2 is a normal byproduct of various metabolic processes that occur within the body. Normal levels of CO_2 in the arteries ($PaCO_2$) are maintained through excretion through the lungs, as the CO_2 diffuses from the pulmonary capillaries through the alveolar capillary membrane and into the alveoli. The movement of gas into and out of the body completes the cycle of CO_2 elimination. However, due to the anatomy of the airways and volumes of the lungs, each breath does not ventilate enough gas to completely clear the CO_2 that resides within the airways. This causes the rebreathing of CO_2 and increases the CO_2 composition that fills the alveoli with each breath. In addition to occupying alveolar space that could be filled with oxygen used in oxygen diffusion, the CO_2 gradient between the alveoli and alveolar capillaries is affected and can contribute to slower diffusion across the alveolar capillary membrane. This will lead to a slower rate of diffusion of CO_2 from the body and contribute to greater CO_2 retention.

A portion of all tidal volume (V_T) is comprised of alveolar ventilation (V_{alv}) and dead space ventilation (V_d). We can define dead space ventilation as the portion of V_T that does not participate in gas exchanged and can be conceptualized as wasted ventilation. The volume of dead space ventilation to alveolar ventilation can be calculated by the equation $V_T = V_d + V_{alv}$. From this equation, it can be understood that each normal breath of V_T is comprised of both V_d and V_{alv} (Intagliata et al., 2020). In a normal healthy individual's tidal breath, a rough estimate of V_d can be determined by using the equation $V_d = 2mL/kg$ of body weight in a healthy adult patient and can comprise roughly a third of the V_T (Quinn, 2021). In the pediatric population, the V_d can reach up to >3mL/kg of body weight, causing the V_d/V_T ratio to be even greater (Numa & Newth, 1996). In the younger pediatric population, it is even more important to consider dead space ventilation at an early age (<1 yr) as the portion of V_T is so much greater due to their proportionally larger head size. (Numa & Newth, 1996). In addition, these neonates are primarily abdominal breathers and depend on diaphragmic movement rather than expansion of the ribs. This leads to the only respiratory compensation a neonate can produce is an increase in respiratory rate and not tidal volume (Hall, 1955).

Physiological dead space is made up of anatomical dead space and alveolar dead space. Anatomical dead space includes the nasopharynx, oropharynx, trachea, and bronchi (Intagliata, 2020). Alveolar dead space is the alveoli that receive ventilation but not perfusion from the alveolar capillaries and thus do not participate in gas exchange. There is a greater risk of hypercapnia when factors contribute to the increased physiological dead space in the pediatric population. Conditions such as malignant hyperthermia, increased carbon dioxide production, and increased tissue oxygen consumption can lead to hypercapnia unless CO_2 can be excreted through respiratory compensation. An increase in $PaCO_2$ can cause an individual to increase their

respiratory rate. As long as the V_d/V_T ratio is the same by maintaining a similar V_T, an individual's minute ventilation as well as dead space ventilation and alveolar ventilation increase as the respiratory rate increases.

In terms of hypercapnia, $PaCO_2$ levels are increased through production of CO_2 and maintained by elimination through ventilation. Ventilation is composed of volume and rate of respirations, which can be measured as total volume moved within a minute, also known as minute ventilation. As mentioned before, a portion of the minute ventilation is dead space. The greater the amount of dead space, the less efficient each breath is in terms of taking in oxygen and eliminating CO_2 (Möller et al., 2017). It can be stated that the more dead space involved, the less CO_2 elimination occurs, and the greater the chance of developing hypercapnia. Following the same logic, by removing dead space with high flow rates, CO_2 retention can be avoided. Otherwise, greater volumes would be necessary to decrease the V_d/V_T ratio, which cannot be achieved with a HFNC device.

In terms of hypoxia, the HFNC can provide a set amount of fraction of inspired oxygen (FiO_2) up to 1.00 while providing high flow rates. By providing a high saturation of oxygen flow to a patient's lungs as well as washing out physiological dead space, hypoxia that is nonrefractory to oxygen therapy can be treated (Papazian et al., 2016). The dead space washout prevents the rebreathing of CO_2 and allows for oxygen rich gas to reach the alveoli and cross into the bloodstream.

The HFNC can also target a temperature of 37°C and provide 100% relative humidity. High flow devices deliver gas at rates much greater than an individual's normal inspiratory rate (Ramnrarayan & Schibler, 2017). This bypasses the normal heating and humidifying abilities of the upper airway as gas moves towards the lungs. Without heat and humidification, the high flow

rates of dry air would deplete tissues and secretions of moisture (Fontanari et al., 1996). This would lead to irritation as well as thicker secretions, causing additional harm to a patient who already requires respiratory support. By heating and humidifying the gas, the bypassed anatomical heating and moisturizing effects can be supplemented and provide comfortable therapy to the patient.

The use of HFNC in adults is routinely administered as an intermediate therapy between the venturi mask and noninvasive positive pressure ventilation (Kwon, 2020). The use of HFNC in pediatrics has gained attention in recent years and has found its way into clinical practice primarily for respiratory support in bronchiolitis patients (Milési et al., 2017). In this in vitro study, we will examine the effects of flow from a HFNC on mean airway pressure in the pediatric population by using a pediatric lung model.

Purpose of the study

This study aimed to examine the impact of increasing flow through a HFNC device on MAP in a pediatric patient by using an in vitro model. It also aimed to compare the effects that different commercial HFNC device has on MAP values by testing multiple HFNC on the same flow settings. Lastly, we examine the effects that breathing pattern has on MAP values in a pediatric in vitro model.

Research Questions

Three study questions drive this study:

1. Does increasing flow through a HFNC device increase MAP?

2. Do HFNC devices produce significantly different MAP values?

3. Do simulated breathing patterns differ in their effect on MAP?

Significance of Study

The current study will contribute to our knowledge of how HFNC devices achieve increases in MAP through the increase of flow rate in the pediatric population, ages 6-12. Moreover, it will provide an understanding of how HFNC devices effect on MAP can vary by manufacturers and how MAP values differ during labored breathing patterns in the pediatric population.

CHAPTER II

REVIEW OF LITERATURE

The review of literature provides background information of multiple aspects of high flow nasal cannulas including: flow therapy, positive pressure therapy, mean airway pressure, HFNC devices, and HFNC device uses in the adult and pediatric population. The databases used to obtain literature included PubMed, Google Scholar, and CINAHL. Key terms were used in the search such as *high flow nasal cannula, dead space ventilation, positive pressure therapy, high flow therapy, low flow therapy,* and *mean airway pressure.* Data from neonatal studies, pediatric studies, and adult studies were included for comparative purposes. Studies included in vitro studies as well as randomized control studies and meta-analyses.

Background Information on HFNC

HFNC therapy is often ordered for patients who are moderately hypoxemic and can benefit from a low amount of positive pressure to stent open the airways and alveoli (Kwon, 2020). Situations where patients can benefit from the use of HFNC include post extubation respiratory support, asthma, respiratory distress, and the prevention of intubation (Coletti et al., 2017). HFNC allows for the delivery of FiO_2 of 1.00 at a flow rate up to 60 (L/min) with a precise temperature of 37°C (Lodeserto, 2018). The benefit of providing a FiO_2 of 1.00 assists patients who are responsive to oxygen therapy and possess a higher flow demand. This allows an escalation of treatment from the venturi mask which can provide higher flows at an exchange for lower FiO_2, or from a nonrebreather mask (NRB) which can provide high FiO_2 at a low flow (Ward, 2013). The HFNC also provides an alternative to patients who are unable to tolerate or properly fit a continuous positive airway pressure (CPAP) mask and require a low amount of positive pressure ventilation (Ward, 2013). One study found that of 620 pediatric subjects that

were given HFNC, only two were documented to discontinue therapy due to discomfort (Coletti et al., 2017).

<center>**Flow**</center>

The delivery of gas therapy generates a flow rate as it moves through a patient's airway. This flow rate can be felt by a patient as the force of gas pushes against the airways, indicating to the patient if sufficient flow is being made. When patients have normal, patent airways, there may be a lower need for high flow rates and instead a greater FiO_2 to treat hypoxemia, or a partial pressure of oxygen (PaO_2) in the arteries less than 80 millimeters of mercury (mmHg) (Ward, 2012). Low flow rates can be accomplished with devices such as the nasal cannula, simple mask, NRB, or a t-piece. An issue with low flow devices is the effect of a patient's effort on atmospheric air entrainment (Lodeserto, 2018). Atmospheric entrainment causes the delivered FiO_2 from the source to drop below the set value, providing the patient with a variable FiO_2 that can be any value below an FiO_2 of 1.00.

When patients have a high flow demand, low flow devices are insufficient to meet a patient's needs. In these instances, a blender set up or high flow device is required to meet and exceed a patient's high flow demand to ensure proper ventilatory support (Nishimura, 2016). High flow devices include the venturi mask, high flow nasal cannula, noninvasive positive pressure devices, and mechanical ventilation. These devices can produce a flow that exceeds a patient's needs even during respiratory distress, when flow and volume demands are increased.

<center>**Positive pressure**</center>

Positive pressure therapy uses an external source to apply positive pressure to a patient's airway or alveoli. Typically, the external source will be a form of gas delivered to the nares or

mouth through an external device such as nasal prongs or mask or through an internal device such as an artificial airway (Ekhaguere et al., 2019).

The pressure achieved in the alveoli during gas delivery is known as plateau pressure (P_{PLT}). P_{PLT} represents the delivered volume's effect of pressure upon the alveoli in the absence of active gas flow and results in the measurement of static compliance (CL_{ST}) of the lung. CL_{ST} is the amount of volume that can be increased for each unit of pressure. Normal values for CL_{ST} in a healthy individual without pulmonary issues are approximately 0.1 liter per centimeter of water (L/cm H_2O). Greater CL_{ST} allows for lower P_{PLT} to be achieved for a given delivered volume. CL_{ST} and P_{PLT} have an indirect relationship. Greater delivered volumes result in greater P_{PLT}. Volume and plateau pressure have a direct relationship. The written formula for CL_{ST} can be seen as $CL_{ST} = \Delta$ volume / (P_{PLT} – PEEP). When the formula is rearranged to isolate P_{PLT}, it shows as $P_{PLT} = (\Delta$ volume / CL_{ST}) + PEEP. Thus, as CL_{ST} decreases or Δ volume increases, P_{PLT} increases.

The maximum pressure achieved in the patient's airway during gas delivery is known as peak airway pressure or peak inspiratory pressure (PIP). PIP is the highest pressure that is measured in the airways and is dependent on the patient's airway resistance (R_{AW}) and the amount of flow passing through the airways (Gali & Goyal, 2003). Greater R_{AW} results in greater PIP. Greater flow results in greater PIP. Both R_{AW} and flow have a direct relationship with PIP.

HFNC creates continuous distending pressure to the pharyngeal airway and a small degree to the peak end expiratory pressure in the airway. This maintains functional residual capacity. In addition, the positive pressure increases the size of the pharyngeal airway and decreases airway resistance during inspiration (Ekhaguere et al., 2019). Low levels PEEP can also be produced by HFNC, which help in preventing alveolar collapse at end expiration. This

improves oxygenation by increasing function residual capacity, improving ventilation-perfusion

matching, and redistributing extravascular lung water (Gali & Goyal, 2003).

Mean airway pressure

As the name suggests, MAP is the average pressure generated over time within the

airway. In terms of airway ventilation, mean airway pressure has been monitored during both

noninvasive and invasive mechanical ventilation. However, as long as there is flow moving

through the airways, a mean airway pressure may also be recorded during ventilation of any sort.

As mentioned above, the variables such as gas flow, CL_{ST}, volume, and R_{AW} impact the pressure

generated during ventilation.

Based on the flow rate set, this device should cause a degree of pressure difference

depending on the set flow rate. One study found that HFNC provides a low amount of upper

airway distending pressure (Ward, 2012). Other studies have compared the amount of PEEP

generated with an open and closed mouth model, finding that open mouth models represent a

severe leak, with a decrease of up to 50% in PEEP (Nielson et al., 2018). The same study found

that flows greater than 20 L/min can cause a PEEP of greater than 10 cm H_2O. These findings

support that higher flows may have an impact on MAP by creating a greater amount of PEEP.

Studies have found that the HFNC does impact PEEP in all age populations, with one study

stating that the flows required to accomplish a PEEP of 6 increases with age (Nielson et al.,

2018). These findings go on to state that to maintain a PEEP of 6 in a small child, flow rates of

12-20 L/min would be required. Many studies have been performed to focus on the uses of

HFNC in the adult population as well as the younger end of the spectrum of the pediatric

population that focuses on neonates and peri neonates. To make matters more difficult, most

research performed on the middle range of the pediatric population that spans between 6-12

years old has very limited research. The absence of scientific literature pertaining to 6–12-year

old's leads practitioners to provide treatment based on evidence that has not been thoroughly

applied to this age range.

**Figure 1** *Vapotherm Precision Flow® HFNC System*

HFNC Devices

The HFNC systems used to compare pressure results include the Vapotherm Precision Flow (Vapotherm, Exeter, New Hampshire) (Figure 1), the Optiflow+ OPT942 (Fisher & Paykel, Auckland, New Zealand) (Figure 2), and the Hudson RCI HFNC (Teleflex, Wayne, Pennsylvania(Figure 4).

HFNC in the Adult Population

In the adult population, the uses of HFNC have been investigated for various clinical conditions and respiratory support. It is commonly used for community acquired pneumonia except in patients with COPD, who would benefit more from non-invasive positive pressure ventilation (NIPPV) (Lodeserto et al., 2018). Compared to NIPPV, HFNC allows for effective coughing and expulsion of secretions, the ability to be

Figure 2 (left) and 3 (right) *Clamping of Optiflow+ HFNC and stands*
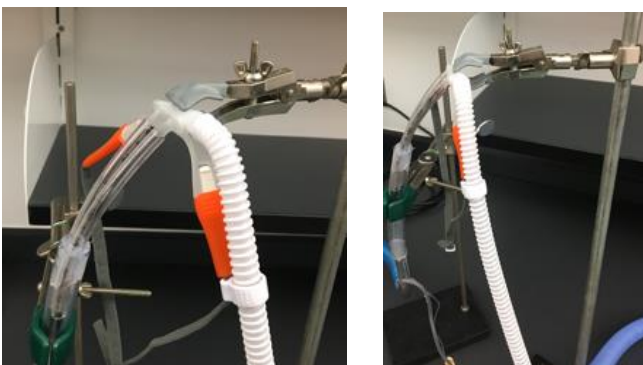
suctioned, as well as provides a more comfortable interface. Numerous studies have been performed to study HFNC in the adult population that compare HFNC to NIPPV and convention oxygen therapy (Frat et al., 2015; Ni et al., 2017; Azoulay et al., 2018). HFNC was compared to

NIPPV and NRB in adult patients with community-acquired pneumonia and found that although

no significant differences were found in intubation rates, HFNC

did show improved results in 90-day all-cause mortality compared

to the NIPPV and NRB (Frat et al., 2015). When compared to

NIPPV and conventional oxygen therapy, HFNC reduced

endotracheal intubation rates in patients experiencing acute

respiratory failure (Ni et al., 2017). Azoulay et al. (2018)

examined HFNC compared to conventional oxygen therapy in

immunocompromised subjects and found that HFNC achieved

improvements in oxygenation. However, HFNC failed to

demonstrate differences in 28-day mortality, intubation rates, and

Figure 4 *Hudson HFNC system with 22 mm corrugated tubing*

hospital length of stay. Although this study conflicts with the previous studies that included

NIPPV, it shows that the effect of HFNC can produce different effects based on the presence of

chronic conditions.

HFNC in the Pediatric Population

The age range of pediatric patients span from one year to eighteen years. Our search

found that the majority of HFNC interventions and comparisons performed in the pediatric

population surrounded the earlier six years of life. In particular, HFNC is primarily used to treat

bronchiolitis in patients two years old and younger (Peterson et al., 2021). The respiratory

support it provides with high flow and heated, humidified gas has led to a decrease in intubation

and length of hospital stay in pediatrics younger than two years old. Further, HFNC therapy has

been successfully utilized in respiratory support to prevent re-intubation (Peterson et al., 2021).

In a study performed by McKiernan et al. (2009) 9% of infants admitted to the PICU with

bronchiolitis required intubation following the implementation of HFNC therapy. Prior to the

implementation of HFNC therapy, intubation rates in the PICU for infants with bronchiolitis was

23% (McKiernan et al., 2009). The study also found that HFNC helped decrease the respiratory

rate compared to alternative respiratory support.

Comparisons between HFNC therapy and nasal continuous positive airway pressure

(nCPAP) in neonates with bronchiolitis were conducted by Metge et al. (2014) and found no

differences in the management of severe bronchiolitis between groups. However, this study only

included a small sample of thirty-four neonates. In a multicentered randomized controlled trial

comparing HFNC and nCPAP, Milési et al (2017) found that HFNC therapy was not as effective

as nCPAP in neonates with acute viral bronchiolitis. When respiratory treatment failed with

HFNC therapy, two-thirds of infants were successfully treated with nCPAP. In terms of tolerance

between the two devices, HFNC therapy was better tolerated due to a higher degree of comfort

that allowed for the infant's unobstructed visual field and unrestricted communication abilities

(Milési et al., 2017).

Ramnarayan & Schibler (2017) stated that in the last decade, HFNC therapy in the

pediatric population has gained popularity. Critically ill children with bronchiolitis, asthma,

respiratory failure, and neuromuscular illnesses have been managed with HFNC therapy. As the

indications for more uses of HFNC broadens, it presents the need to better understand how

HFNC device produce these benefits and if there are risks involved (Sorkness et al., 2019). A

benefit of HFNC is the amount of pressure it can provide to a patient's airway, specifically the

pharyngeal pressure and peak end expiratory pressure (PEEP) (Baudin et al., 2016). The amount

of pressure found varies between studies. Baudin et al. (2016) reports that a PEEP of 2-7 cm H_2O

can be generated depending on the flow, nasal cannula size, and if the mouth is open or closed.

Schmid et al. (2017) sites that at flow rates of 1-6 L/min and open mouth compared to closed mouth, the distending pressure does not exceed 2 cm H_2O and 10 cm H_2O, respectively.

One of the most important aspects of this research is to provide an association between the increase of flow through a HFNC and its impact on MAP since airway pressures cannot be monitored using a HFNC system. Although flow rate, FiO_2, heat, and humidification can be set this high flow system cannot measure the airway pressure like NIPPV and mechanical ventilation can, making this unknown pressure potentially hazardous. Some risks identified for HFNC include pneumothorax, pneumomediastinum, or clinically important epistaxis. Three cases were identified retrospectively where pediatric patients experienced serious air leak syndromes related to HFNC therapy. While 2 cases involved a patient less than two-years old, the third case involved a 16-year-old male. On a flow rate of 20 L/min, this patient developed pneumomediastinum and subcutaneous air leaks. Although other airway pressure therapies were implemented, the exact cause of injury includes the effect of flow from the HFNC (Hedge & Prodhan, 2013). Chang et al. (2011) found that HFNC devices produce much higher pressures compared to a CPAP device at all flow rates ranging from 1 to 8 L/min. CPAP generated approximately 30 cm H_2O compared to HFNC at greater than 120 cm H_2O when set at 8 L/min. If these results are accurate, HFNC flows should be examined closely to ensure proper settings are chosen for at risk patients.

This lack of research itself stands as a reason for further research regarding the middle pediatric population. This bench study will bridge the gap of knowledge for HFNC therapy between adult and the younger pediatric population, as well as ensure that a continuum of understanding of HFNC devices exists.

Conclusion

There is insufficient data on the effects of HFNC in the pediatric population, specifically

the ages 6-12-years-old. While numerous large-scale studies have been conducted in the neonatal

population and adult population, the same initiatives have not been taken for the middle pediatric

population. HFNC can enhance oxygenation provide a small amount of ventilatory support

through dead space washout. However, the high flows generated are unmeasured during oxygen

therapy and places patients at an increased risk of barotrauma. For this reason, this study looks to

evaluate the effects of increasing flow through HFNC devices on MAP in our study population

to expand our knowledge of flow on pressure gradients.

CHAPTER III

METHODS

The goal of this study was to observe if pressure gradients were generated by the HFNC

on a spontaneous breathing pediatric lung model. Three study questions directed the research

methods: (1) Does greater flow through a high flow nasal cannula increase MAP? (2) Do the

devices used in this study produce statistically different values? (3) Is greater MAP produced

during simulated unlabored breathing compared to labored breathing pattern?

The focus was to investigate whether or not an increased flow rate would also increase

the MAP. To simulate a spontaneous breathing patient, a system needed to be constructed to

provide the negative pressure associated with spontaneous breaths. To do this, a double lung

model, the Michigan Instruments Labs (MIL) Dual Adult TTL Lung (Michigan Instruments, Inc.

Grand Rapids, Michigan) was utilized with a board to connect both lungs to move as a single

unit. Attached to one side of the double lung model would be a ventilator on assist control

volume control settings to create a negative pressure dynamic on the opposing lung model. The

ventilator was used in this setting to provide a precise tidal volume, respiratory rate, and time of

inspiration and expiration. The board that is clamped to both sides of the lung model ensure that

synchronous movement occurs as the ventilator provides mandatory breaths to Side A. As Side

A rises due to positive pressure from the ventilator, Side B will also rise due to the clamping of

the board to both sides of the test and training lung and will therefore generate negative pressure

inside of Side B. Side B of the double lung model would receive flow from the pediatric HFNC

circuit.

The HFNC circuit will provide flow to the lung model through a constructed pair of nares

model using two 6.0 mm endotracheal tube (Medtronic, Dublin, Ireland) (ETT) trimmed to

exclude the cuff and fitted into an 8.5 mm ETT (Medtronic, Dublin, Ireland). This produced an

upper airway model that consisted of two cuff-less 6.0 mm ETT to be paired together and

secured within the 8. 5mm ETT. Silicon sealant was used in the space between the two 6.0 mm

ETT and the 8.5 mm ETT to secure and seal the gaps. The size of the ETT was selected so the

inner lumen diameter would be the approximate size of the nares of a pediatric patient that we

used for this study.

Stands with clamps was positioned to hold the fabricated airway and HFNC device in

place so the nasal prongs are properly fit within the in vitro nares as seen in Figures 1 and 2.

Adjustments were made so the clamps did not compress and

Figure 5 *Auxiliary pressure sensor is attached between the fabricated airway and the TTL*

jeopardize the patency of either piece of equipment. An auxiliary

pressure sensor was attached to the circuit on Side B leading from the

fabricated airway to the TTL to measure airway pressures as seen in

Figure 5. For the Hudson RCI and Optiflow HFNC, a high flow

Figure 6 *MR290 Auto-fill Chamber and Heated Breathing Tube with MicroCell Technology used to connect HFNC devices to high flow Thorpe tube*

Thorpe tube (5-75 lpm) was utilized and

connected to an adaptor to the Fisher and

Paykel MR290 Auto-fill Chamber and Heated Breathing Tube with

MicroCell Technology as seen in Figure 6.

The age range of pediatric patients span from one year to

eighteen years. For the purposes of this study, we have chosen the

age range to encompass the middle range of the pediatric population,

ages 5-12. This age range was chosen based off the study conducted

by Coletti et al. (2017) that found that the majority of patients that

were managed with HFNC tended to be < 12 years old. The

distribution between age groups were equal. The Vapotherm guidelines recommend that

pediatric/adult small HFNC be used for the age range of 6-12 years old. The outer diameter of

the pediatric/adult small HFNC is 2.7mm and can supply 5-40L/min. Each of the constructed

nares would have an inner diameter greater than 5.73 mm to simulate the nares of our target

population. For this study, a size 6.0 mm ETT was used to simulate a single nare, so two 6.0 mm

ETT were used.

Lung Model

The in vitro lung model used for this study was the Michigan Instruments Labs (MIL) Dual Adult TTL Lung as seen in Figure 7. The Dual Adult TTL has two independent lungs that allow for independent ventilation. Compliance for both sets of lungs was set to 0.1 L/cmH$_2$O. No additional resistance was included for this study.

Figure 7 *Dual Adult TTL with clamped board*

Note. Side A on the left of the TTL is ventilated through the Hamilton-G5. Side B on the right of the TTL is receiving flow through the HFNC devices. The board clamped across both sides of the TTL simulated negative pressure ventilation on Side B.

Figure 8 *Hamilton-G5 ventilator*

Note. The Hamilton-G5 ventilator provides ventilation to Side A of the TTL and also shows pressure reading from the flow generated from the HFNC systems on Side B.

Ventilator

The Hamilton-G5 ventilator as seen in Figure 8 (Hamilton Medical, Inc. Reno, Nevada) was utilized for this study. Ventilator settings were chosen to mimic pediatric ventilation. Two parameters to simulate

labored and non-labored breathing were used. Non-labored parameters were set as followed: tidal volume of 170 mL, respiratory rate of 20, PEEP of 0, FiO_2 of 0.21, and flow rate of 20.4 L/min to produce an I:E ratio of 1:2.8. Labored parameters were set as followed: tidal volume of 170 mL, respiratory rate of 40, PEEP of 0, FiO2 of 0.21, and flow rate of 40.8 L/min to produce an I:E ratio of 1:2.8.

Tidal volumes were determined by calculating the expected tidal volumes for an average height ten-year old pediatric, regardless of gender. According to Bonthuis et al. (2012), the average ten-year old is approximately 140 cm. To determine the IBW of a 140 cm child, we used the formula provided by Bilharz et al. (2018) as stated: IBW (male) = [(18.41 – 0.096 (age)) + (0.00087 (age^2))] x $(height^2)$. For a 140 cm child, the IBW was calculated to be 34.37 kg. Based on the findings from Santschi et al. (2007)97 pediatric intensivists recommended a tidal volume of 5mL/kg for a ten-year old. The tidal volume was calculated to be 171.85 mL for a 140 cm child. For this study, a tidal volume of 170 mL will be used for ease of controls. Ventilator calibration will be performed per manufacturer guidelines prior to testing.

Data Collection

Protocols described in Appendix A and Appendix B were used for data collection monitored by the Hamilton-G5 ventilator. The PEEP and peak inspiratory pressure (PIP) were recorded for this study. Warm-up periods included in the protocols were performed prior to the recording of pressures from 20 breaths.

MAP was calculated using the recorded PIP and PEEP, as well as the time constants of the recorded breaths. By using the formula MAP = [(T_I x PIP) + (T_E x PEEP)] / T_{TOT} where T_I represents time of inspiration, T_E represents time of expiration, and T_{TOT} represents the total cycle time of a complete respiration, we calculated the MAP for all breaths. Under normal

breathing conditions, an individual inspires by moving their diaphragm downwards towards their pelvis. This causes negative pressure to be produced within the thoracic cavity and within the airways. Since we are using an in vitro method in this study, we will be utilizing the Hamilton-G5 ventilator to produce the breaths that a normal person would create.

The Hamilton-G5 ventilator can provide a precise amount of volume, pressure, and flow while measuring these values. For the calculation mentioned above that is used to calculate MAP, we are unable to identify the T_I and T_E in a normal spontaneously breathing person. The ventilator will therefore be able to produce a measurable and concise amount of flow and pressure for the exact time that we set it to. On the Hamilton-G5 ventilator, we can set the T_I by going into the ventilator settings, clicking on peak flow setting, and adjusting your flow rate. The ventilator is capable of calculating the set inspiratory time and expiratory time, as well as the ratio of inspiratory time and expiratory time based on the ventilator peak flow rate setting and the tidal volume setting. Since the T_I and T_E are provided to us, we can use those values in the calculation for MAP. Using the auxiliary pressure sensor attached from the ventilator to the circuit between the fabricated airway and Side B of the test lung, we can obtain the peak airway pressure and PEEP in the spontaneous breathing model. The peak airway pressure and PEEP can then be used in the calculation to determine true MAP for each breath.

Data Analysis

SPSS for Windows (version 26.0) was used to analyze the data. The analysis performed on the data included descriptive statistics, two-way ANOVA, and a Bonferroni test. Descriptive statistics were used to assess the MAP values amount different flow rates, breathing patterns, and HFNC devices. Two-way ANOVA was used to compare differences in MAP values among

different flow rates and breathing patterns for different HFNC devices. The Bonferroni

correction was used for the post-hoc test. A p-value of less than 0.05 was considered significant.

CHAPTER IV

RESULTS

The focus of this study was to determine if the effect of greater flow through a HFNC resulted in an increased MAP. In addition, this study was constructed to determine if the pressure outputs of the three commercial devices at the designated flow rates were statistically different. Finally, this study investigated whether MAP results were different between breathing patterns. 360 pressure measurements were recorded and calculated for analysis. 20 measurements were taken for each grouping of HFNC systems, flow rates, and simulated breathing patterns for a total of 18 combinations. Figures 9 and 10 show an upward trend in average MAP across devices as the flow rate increases for both simulated unlabored and labored breathing patterns.

Figure 9 *Device Comparison for average MAP for simulated unlabored breathing pattern*
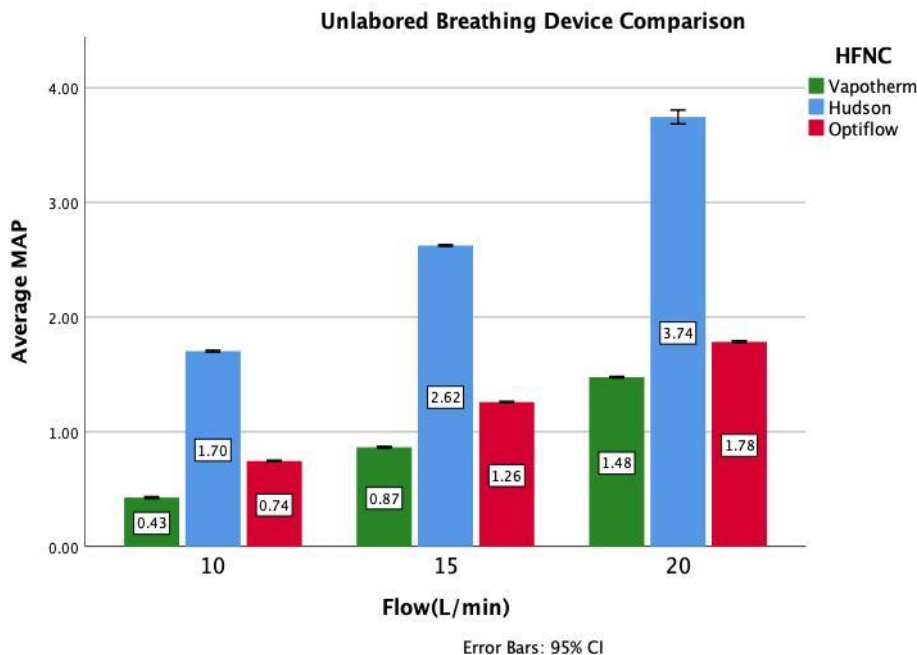
Note. All comparisons were significantly different. $p < 0.001$.

Figure 10 *Device Comparison for average MAP for simulated labored breathing pattern*
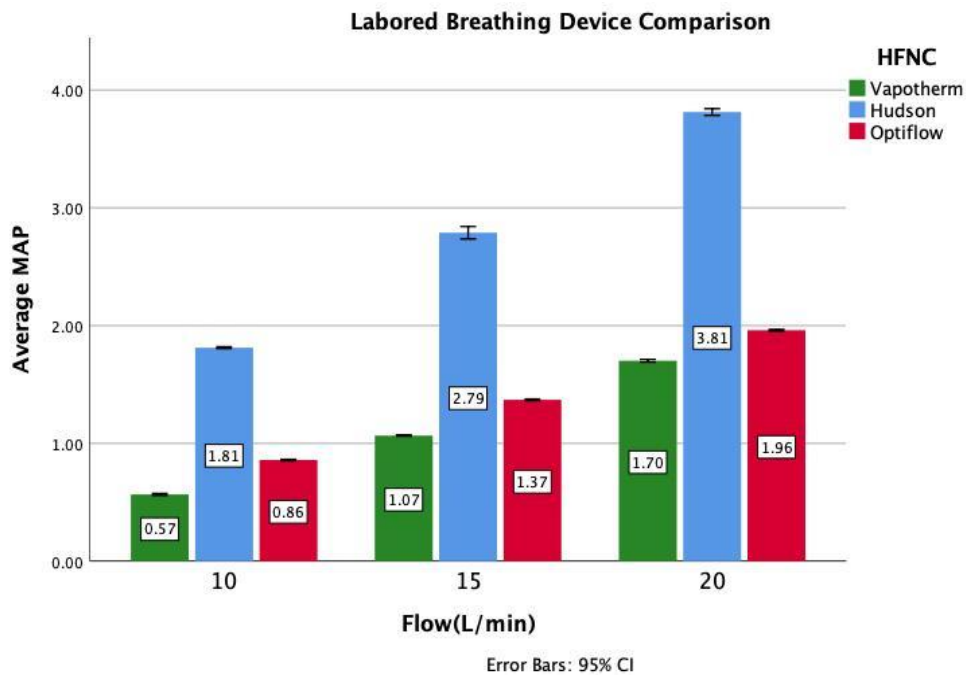
Note. All comparisons were significantly different. $p < 0.001$.

Does increasing flow through a HFNC device increase MAP?

The first question was addressed by using a two-way ANOVA analysis for each simulated breathing pattern and comparing the effects of each flow rate for each HFNC system. There was a statistically significant interaction between the effects of HFNC device and flow rate, $F_{(4,342)} = 22.088$, $p < 0.05$, HFNC device and simulated breathing mode, $F_{(2,342)}$, $p < 0.05$, flow rate and breathing mode, $F_{(2,342)}$, $p = 0.02$, and HFNC, flow rate, and simulated breathing mode, $F_{(4,342)}$, $p < 0.05$. Our post hoc analysis show differences in MAP between each flow rate for all three HFNC, $p < 0.05$. Results can be seen in Table 1.

Table 1 2-way ANOVA performed comparing the effects on MAP between all HFNC devices, all flow rates, and all breathing patterns

Source	Type III Sum of Square	df	Mean Square	F	Sig.
Corrected Model	335.054	17	19.709	9634.873	.000
Intercept	1037.777	1	1037.777	507321.755	.000
HFNCDevice	204.159	2	102.079	49901.917	.000
FlowLMin	116.980	2	58.490	28593.033	.000
BreathingMode	1.897	1	1.897	927.210	.000
HFNCDevice*FlowLmin	11.817	4	2.954	1444.255	.000
HFNCDevice*BreathingMode	.090	2	.045	22.088	.000
FlowLmin*BreathingMode	.027	2	.013	6.593	.002
HFNCDevice*FlowLmin*BreathingMode	.085	4	.021	10.366	.000
Error					
Total					
Corrected Total					

Note. R squared = .998 (Adjusted R Squared = .998)

Dependent variable: MAP

Do HFNC devices produce significantly different MAP values?

The second question was addressed by using a two-way ANOVA analysis for each simulated breathing pattern and comparing the effects of each HFNC system at each flow rate. There was a statistically significant interaction between the effects of HFNC device and flow rate, $F_{(4,342)} = 22.088$, $p < 0.05$, HFNC device and simulated breathing mode, $F_{(2,342)}$, $p <$

0.05, flow rate and breathing mode, F (2,342), $p = 0.02$, and HFNC, flow rate, and simulated

breathing mode, F (4,342), $p < 0.05$. Our post hoc analysis show differences in MAP between

each device for all three flow rates, $p < 0.05$. Results can be seen in Table 1.

Do simulated breathing patterns differ in their effect on MAP?

The third question was addressed by using an independent T-test for each HFNC system

at a single flow, compared between unlabored and labored groups. A total of the nine

independent T-test analyses performed: three for each HFNC system for each of the three flow

rates. There is a significant difference in MAP between simulated unlabored and labored

breathing groups for all three HFNC systems at all three flow rates, $p < 0.05$.

Summary

In conclusion, this study was able to answer three questions. Figure 1 shows that as flow

increased from 10 to 15 to 20 L/min, a greater MAP was produced. For all devices and simulated

breathing patterns, 20 L/min produced the greatest amount of MAP. Statistical analysis showed a

significant difference between devices on the amount of MAP produced. In addition, a

significant difference was found between MAP produced between simulated labored and

unlabored breathing patterns. The simulated labored breathing pattern on average produced a

greater amount of MAP than the simulated unlabored breathing pattern.

CHAPTER V

DISCUSSION

This study was designed to answer three questions. The first question was to determine if there were a positive association between greater flow rates through the HFNC and increased MAP. The second question was to determine if HFNC devices produced statistically different MAP values. The third question was to determine if the average MAP was greater during simulated unlabored breathing patterns or simulated labored breathing patterns. This study made three separate comparisons within the following variables to determine if they caused a significant difference on MAP: flow rates, HFNC devices, and simulated breathing patterns.

Does increasing flow through a HFNC device increase MAP?

Using the pediatric in vitro model, 20 PIP recordings were measured using three HFNC systems: Vapotherm, Hudson, and Optiflow+. The average recorded MAP produced a value greater than 0 cm H_2O for all three flow rates. The average MAP rose with each increase in liter flow in increments of 5 liters per minute. Therefore, we have found that HFNC increases MAP and greater flow through the HFNC produces greater MAP. Since the amount of volume being provided by the ventilator was set to 170 mL, the amount of airway pressure would be the product of lung compliance and tidal volume. Using the formula of MAP = [(T_I x PIP) + (T_E x PEEP)] / T_{TOT}, we can determine that as PIP increases, MAP increases. Based on the results of this study, the greater the flow used through the HFNC, the greater the PIP. Since PIP increased with greater flow, it can be concluded that MAP increases with greater flow.

Nielson et al. (2017) support that HFNC generate PEEP as the flow rate increases and are capable of generating a PEEP of 6 cm H_2O at a flow rate of 12-20 L/min. This would explain the increases in MAP as flow rate increased, since PEEP is part of the equation to calculate MAP.

Nielson et al.'s study results differed from this study when comparing measured pressures. They claimed that the Vapotherm HFNC produced higher pressures than the Optiflow HFNC, while this study showed that Vapotherm produced the lowest pressures. In addition, that study concluded that as flow increased, CO_2 clearance also increased until a change point was reached (Nielson et al. 2017).

For clinical application, the positive association of increasing the flow through a HFNC device to obtain a higher MAP is an intuitive concept. This study contributes to the body of knowledge that this concept applies to the pediatric population as well. When working with patients, increasing the flow through a HFNC device will produce a greater amount of MAP, which has been shown to improve oxygenation status.

Do HFNC devices produce significantly different MAP values?

The three HFNC systems were compared at different flow rates for a side-by-side comparison. Of the three commercial systems, the Hudson HFNC system produced the highest MAP at each flow rate. The greatest MAP produced was at the flow rate of 20 L/min with the Hudson HFNC system at 3.83 cm H_2O during labored breathing and 3.8 cm H_2O during unlabored breathing with an average MAP of 3.81 cm H_2O and 3.7 cm H_2O respectively. The Vapotherm HFNC system at the highest flow produced a maximum MAP of 1.78 cm H_2O during labored breathing and 1.48 cm H_2O during unlabored breathing with an average MAP of 1.7 cm H_2O and 1.5 cm H_2O respectively. The Optiflow+ HFNC system at 20 L/min flow produced a MAP of 1.96 cm H_2O during labored breathing and 1.78 cm H_2O during unlabored breathing with an average MAP of 2.0 cm H_2O and 1.83 cm H_2O respectively. Two-way ANOVA showed significant differences as liter flow increased. Upon comparison of the three commercial HFNC systems, the Hudson produced the greatest MAP at all flows and simulated breathing patterns.

Upon further investigation, we measured the nasal prong diameters of each HFNC device to determine if there was an indication as to what could cause the MAP differences. Per manufacturer recommendations, HFNC prongs should take up no more than 50% of the area of a patient's nare. Using a caliper, we found the outer diameters of the Vapotherm (4.05 mm), Hudson (4.93 mm), and Optiflow+ (4.58 mm). When calculating the area each HFNC nasal prong occupied, 12.882 mm^2, 19.089 mm^2, and 16.475 mm^2 respectively. When compared to the 6.0 mm ETT area of 27.274 mm^2, we calculated the area percentage of nasal prong displacement for the Vapotherm (47.2%), Hudson (70.0%), and Optiflow+ (60.4%). When comparing the amount of area displacement to the average MAP values, similar comparisons can be made as the Hudson HFNC nasal prongs displaced the largest portion of the 6.0 mm ETT and also produced the greatest MAP value while the Vapotherm HFNC nasal prongs displaced the smallest portion of the 6.0 mm ETT and produced the lowest MAP value. The Hudson HFNC may have also produced the greatest expiratory resistance, contributing to a small degree of end expiratory lung recruitment. These findings differ from the study performed by Nielsen et al. (2018) where they speculate that smaller bore cannula produced a higher flow velocity. An in vitro study also confirmed that increases in leaked flow resulted in decreased pressure readings (Ejiofor et al., 2019). This supports that smaller nasal prongs allow for larger leaks and decreased pressure generation.

Understanding the different amounts of MAP generated by different devices is a consideration that must be accounted for in the clinical setting. If one device produced significantly different pressures than another, the clinician should be prepared to adjust the devices their facility has in stock in order to achieve the same MAP. Since HFNC systems do not provide a pressure measurement, this knowledge is even more crucial to understand (Schmid et

al., 2017). This study does not utilize precise flow delivery systems for two devices, as

mentioned in the limitations. For that reason, a repeated study with proper flow delivery systems

should be conducted to obtain more accurate results.

Do simulated breathing patterns differ in their effect on MAP?

To determine if breathing patterns impacted MAP, we looked at each HFNC device and

compared its values against itself at the same flow rate but between breathing patterns. We

utilized the independent T-test to analyze the results for all HFNC devices at each flow rate. The

analysis showed significant differences in MAP between simulated unlabored and labored

breathing groups for all HFNC devices at each flow rate ($p < 0.05$). The importance of this

finding is that the efficacy of the HFNC devices during increased respiratory rates. If the MAP

generated during labored breathing produced decreased values, HFNC devices would not be

effective in generating increased MAP during tachypneic breathing. In contrast, since the MAP

generated during simulated labored breathing were greater than during normal unlabored

breathing, the HFNC devices are more effective during tachypneic episodes.

McKiernan et al. (2010) found that infants in respiratory distress showed clear

improvements in respiratory rate within 90 minutes of HFNC therapy if HFNC were to be

successful. Infants showed a decrease in RR by 14 breath per minute (bpm) if HFNC was

effective compared to 1 bpm if therapy was ineffective and required an escalation in therapy.

This window allows for clinical teams to anticipate effectiveness of therapy quickly and alter

courses if necessary (McKiernan et al., 2010).

Moving forward, understanding the degree of MAP generated during increased

respiratory rates compared to respiratory rates within normal limits can drive treatment plans.

Since the MAP is greater during higher respiratory rates, the amount of flow may be decreased if

there is a risk of barotrauma with the patient. In addition, if a patient is started on a HFNC device during a tachypneic episode, flows can be increased following the episode to maintain the same amount of MAP. Dead space washout also normalizes gases, and therefore reduces the drive behind the increased work of breathing (Ejiofor et al., 2019). Understanding the dynamics of HFNC on MAP during different respiratory rates can explain differences in oxygen saturation when HFNC settings are not changed and should be considered when evaluating treatment effectiveness.

Limitations

There are several limitations evident in this study. The following limitations have been identified and considered by the researcher for this study.

1. In vitro results generalize the potential findings that can be expected in the normal population.

2. The fabricated in vitro model is not physiologically correct. The material used does not contain the same characteristics of an actual person's nasal cavity or airway and can produce different values.

3. The fabricated in vitro model may affect the flow of gas through the airway in a manner unlike the normal airway of an actual person. The airway in this study may produce greater or less turbulence than in an actual person as this information was not measured for comparison. Normal airways converge into a single airway at the oropharynx and contain a variety of structures that produce resistance against flow such as the nasal turbinates.

4. The fitting of the HFNC may not have been appropriate for the diameter size of the fabricated in vitro model used. Per manufacturer speculations, the diameter of the nasal

prongs should not exceed 50% of the nares. For this study, we used a single fabricated in

vitro model for the nares and chose the HFNC system that were recommended for this

age group. Different sizes nasal prongs may affect the amount of air entrainment and

influence the amount of flow and pressure produced by each device.

5. No humidity was included in this study. Although these HFNC are constructed to

produce 100% relative humidity, no humidity was included from the patient side or from

the flow being delivered to the patient. The delivered dry air may produce a different

flow dynamic than humidified air, and a humidified airway may produce less resistance

than dry air (Fontanari et al., 1996).

6. No heat was used in this study. In addition to humidification, no heat was applied from

the patient side, nor the flow delivered. Dry air delivery may produce a different flow

dynamic than heated, humidified air, and heated, humidified from the patient side may

produce greater resistance than dry air.

7. No flow sensor was utilized. Although flow was set digitally on the Vapotherm HFNC

system, a high flow Thorpe tube was used to produce flow with the Hudson and

Optiflow+ HFNC systems. This may produce different values in a repeated study and

can affect results.

8. The V_T used in this study is based on the average height of a ten-year old child, then

calculated to determine IBW and multiplied to determine ideal tidal volumes per kg.

Height for this age group can vary upon gender and beginning of puberty. V_T may be

different compared to other studies if volumes were determined another way. Further,

during an exacerbation, V_T may be increased or decreased depending on the clinical

condition of the patient. Rate was the only variable manipulated to represent a

tachypneic patient.

9. The fabricated in vitro model does not consider an open mouth condition. Air

   entrainment and leaks are common when the mouth is open. This study only utilizes a

   nasal airway directly connected to a test lung.

Need for further research

Additional research on HFNC systems should be conducted to produce a thorough

understanding in pediatric patients. Identifying the amount of PEEP that HFNC systems can

produce with these settings can further the advanced knowledge we have about HFNC in the

pediatric population. To calculate the PEEP produced in a reproduced study, the researcher can

measure the MAP in addition to the PIP and subtract the calculated MAP from the actual MAP.

The difference should be divided by T_{TOT} and divided by T_E to obtain the PEEP produced by a

HFNC system.

A fabricated model that takes into account an open mouth model may produce additional

insight. Patients during exacerbations may mouth breathe to achieve greater ventilation and

inspiratory flow. For these individuals, the calculated MAP will not be accurate or reflect the

actual pressures generated by the HFNC system.

A repeated study may consider including humidification and heat to discover if these

characteristics produce different results. In addition, a flow sensor in the circuit on the HFNC

systems side can allow for accurate flows to be set for the Hudson and Optiflow+ HFNC

systems. In addition, taking measurements for the airway without a HFNC system attached

would provide for a control group to comparison.

Conclusion

HFNC systems are deemed one of the most effective non-invasive oxygenation devices available. These systems require quick setup and provide a precise measurement of flow and FiO_2 that allows for concise care management. The flow delivers gas at a higher rate, applying pressure against the airway. During expiration, the continuous flow into the patient's lungs causes resistance to the expiratory flow, producing increased pressure in the airways greater than without continuous flow during expiration. This assists in conditions where radial traction is decreased, or when secretions in the airways collapse due to the high expiratory flow. Although this pressure produced by the HFNC is minimal, it can help in situations where patients require a low degree of expiratory airway resistance.

In addition to precise flow and FiO_2, the HFNC systems can provide heat and humidification to ensure the delivery of oxygen to a patient is comfortable and humidified. By meeting and exceeding the patient's requirements for oxygenation, flow, heat, and humidification, there is a greater tolerance by patients to adhere to treatment. One of the greatest obstacles to another highly effective non-invasive oxygenation device, the NIPPV mask, is the discomfort that is associated with these masks, ofttimes leading to a discontinuation of therapy and worsening conditions. Comfort is certainly an advantage of the HFNC systems, and the higher patient tolerance reflects that.

This study shows that HFNC can produce an increased MAP and PIP as the flow rate is increased. As a direct relationship, as flow rate increases, MAP and PIP increase. The determination if the increase in PIP is due to the production of PEEP cannot be determined from the measurements obtained in this study. As a highly adhered to oxygenation and heated

humidification device, the HFNC systems allow for concise care management of patients

requiring oxygen therapy.

REFERENCES

Azoulay, E., Lemiale, V., Mokart, D., Nseir, S., Argaud, L., Pène, F., Kontar, L., Bruneel, F.,

  Klouche, K., Barbier, F., Reignier, J., Berrahil-Meksen, L., Louis, G., Constantin, J. M.,

  Mayaux, J., Wallet, F., Kouatchet, A., Peigne, V., Théodose, I., Perez, P., … Demoule,

  A. (2018). Effect of High-Flow Nasal Oxygen vs Standard Oxygen on 28-Day Mortality

  in Immunocompromised Patients With Acute Respiratory Failure: The HIGH

  Randomized Clinical Trial. JAMA, 320(20), 2099–2107.

  https://doi.org/10.1001/jama.2018.14282

Bilharz, J. R., Wheeler, C. R., Walsh, B. K., & Smallwood, C. D. (2018). A Comparative

  Analysis of Ideal Body Weight Methods for Pediatric Mechanical Ventilation.

  Respiratory care, 63(9), 1079–1084. https://doi.org/10.4187/respcare.06021

Baudin, F., Gagnon, S., Crulli, B., Proulx, F., Jouvet, P., & Emeriaud, G. (2016). Modalities and

  Complications Associated With the Use of High-Flow Nasal Cannula: Experience in a

  Pediatric ICU. *Respiratory Care*, 61(10), 1305–1310. doi:10.4187/respcare.04452

Bonthuis, M., van Stralen, K. J., Verrina, E., Edefonti, A., Molchanova, E. A., Hokken-Koelega,

  A. C., Schaefer, F., & Jager, K. J. (2012). Use of national and international growth charts

  for studying height in European children: development of up-to-date European height-

  for-age charts. *PloS one*, 7(8), e42506. https://doi.org/10.1371/journal.pone.0042506

Coletti, K. D., Bagdure, D. N., Walker, L. K., Remy, K. E., & Custer, J. W. (2017). High-Flow

  Nasal Cannula Utilization in Pediatric Critical Care. *Respiratory care*, 62(8), 1023–1029.

  https://doi.org/10.4187/respcare.05153

Duprez, F., Bruyneel, A., Machayekhi, S., Droguet, M., Bouckaert, Y., … & Gregory Reychler.

  (2019). The Double-Trunk Mask Improves Oxygenation During High-Flow Nasal

Cannula Therapy for Acute Hypoxemic Respiratory Failure. *Respiratory care*, 64 (8)

908-914; https://doi.org/10.4187/respcare.06520

Ekhaguere, O., Patel, S., & Kirpalani, H. (2019). Nasal intermittent mandatory ventilation versus

nasal continuous positive airway pressure before and after invasive ventilatory support.

Clinics in perinatology. doi: 10.1016/j.clp.2019.05.004

Frat, J., Thille, A., Mercat, A., Girault, C., Ragot, S., Perbet, S., Prat, G., Boulain, T., Morawiec,

E., Cottereau, A., Devaquet, J., Nseir, S., Razazi, K., Mira, J., Argaud, L., Chakarian, J.,

Ricard, J., Wittebole, X., Chevalier, S., . . . Robert, R. (2015). High-Flow Oxygen

through Nasal Cannula in Acute Hypoxemic Respiratory Failure. *N Engl J Med* 2015;

372:2185-2196. https://doi.org/10.1056/NEJMoa1503326

Fontanari, P., Burnet, H., Zattara-Hartmann, M. C., & Jammes, Y. (1996). Changes in airway

resistance induced by nasal inhalation of cold dry, dry, or moist air in normal individuals.

Journal of applied physiology (Bethesda, Md. : 1985), 81(4), 1739–1743.

https://doi.org/10.1152/jappl.1996.81.4.1739

Gali, B., & Goyal, C. 2003. Positive pressure mechanical ventilation. *Emergency medicine

clinics of north America*, *21*(2), 453-473. Doi10.1016/s0733-8627(03)00006-3

Gehlbach, J., Miller, A., Hornik, C., & Cheifetz, I. (2020). Dead Space to Tidal Volume Ratio Is

Associated With Higher Postextubation Support in Children. *Resp Care, 65* (11) 1721-

1729. https://doi.org/10.4187/respcare.07351

Hall, J. (1955). The physiology of respiration in infants and young children. *Proceedings of the

Royal Society of Medicine* 48 (761).

Hedge, S., & Prodhan, P., (2013). Serious air leak syndrome complicating high-flow nasal

cannula therapy: a report of 3 cases. *Pediatrics, 131*(3), e939-e944.

https://doi.org/10.1542/peds.2011-3767

Intagliata, S., Rizzo, A., & Gossman, W. G. (2020). Physiology, Lung Dead Space. *StatPearls*.

StatPearls Publishing.

Kang, B. J., Koh, Y., Lim, C. M., Huh, J. W., Baek, S., Han, M., Seo, H. S., Suh, H. J., Seo, G.

J., Kim, E. Y., & Hong, S. B. (2015). Failure of high-flow nasal cannula therapy may

delay intubation and increase mortality. Intensive care medicine, 41(4), 623–632.

https://doi.org/10.1007/s00134-015-3693-5

Kwon J. W. (2020). High-flow nasal cannula oxygen therapy in children: a clinical review.

Clinical and experimental pediatrics, 63(1), 3–7. https://doi.org/10.3345/kjp.2019.00626

Lodeserto, F. J., Lettich, T. M., & Rezaie, S. R. (2018). High-flow Nasal Cannula: Mechanisms

of Action and Adult and Pediatric Indications. *Cureus*, *10*(11), e3639.

https://doi.org/10.7759/cureus.3639

McKiernan, C., Chua, L. C., Visintainer, P. F., & Allen, H. (2010). High flow nasal cannulae

therapy in infants with bronchiolitis. *The Journal of pediatrics*, 156(4), 634–638.

https://doi.org/10.1016/j.jpeds.2009.10.039

Milési, C., Essouri, S., Pouyau, R., Liet, J. M., Afanetti, M., Portefaix, A., Baleine, J., Durand,

S., Combes, C., Douillard, A., Cambonie, G., & Groupe Francophone de Réanimation et

d'Urgences Pédiatriques (GFRUP) (2017). High flow nasal cannula (HFNC) versus nasal

continuous positive airway pressure (nCPAP) for the initial respiratory management of

acute viral bronchiolitis in young infants: a multicenter randomized controlled trial

(TRAMONTANE study). Intensive care medicine, 43(2), 209–216.

https://doi.org/10.1007/s00134-016-4617-8

Miller, A., Haynes, K., Gates, R., Zimmerman, K., Bartlett, K., … & Kyle J Rehder. (2020).

Initial Modified Pulmonary Index Score Predicts Hospital Length of Stay for Asthma

Subjects Admitted to the Pediatric Intensive Care Unit. *Respiratory Care*, 65 (9) 1227-

1232; https://doi.org/10.4187/respcare.07396

Möller, W., Feng, S., Domanski, U., Franke, K. J., Celik, G., Bartenstein, P., Becker, S., Meyer,

G., Schmid, O., Eickelberg, O., Tatkov, S., & Nilius, G. (2017). Nasal high flow reduces

dead space. *Journal of applied physiology*, 122(1), 191–197.

https://doi.org/10.1152/japplphysiol.00584.2016

Ni, Y. N., Luo, J., Yu, H., Liu, D., Ni, Z., Cheng, J., Liang, B. M., & Liang, Z. A. (2017). Can

High-flow Nasal Cannula Reduce the Rate of Endotracheal Intubation in Adult Patients

With Acute Respiratory Failure Compared With Conventional Oxygen Therapy and

Noninvasive Positive Pressure Ventilation?: A Systematic Review and Meta-analysis.

Chest, 151(4), 764–775. https://doi.org/10.1016/j.chest.2017.01.004

Nielsen, K. R., Ellington, L. E., Gray, A. J., Stanberry, L. I., Smith, L. S., & DiBlasi, R. M.

(2018). Effect of High-Flow Nasal Cannula on Expiratory Pressure and Ventilation in

Infant, Pediatric, and Adult Models. *Respiratory care*, 63(2), 147–157.

https://doi.org/10.4187/respcare.05728

Nishimura M. (2016). High-Flow Nasal Cannula Oxygen Therapy in Adults: Physiological

Benefits, Indication, Clinical Benefits, and Adverse Effects. *Respiratory care*, 61(4),

529–541. https://doi.org/10.4187/respcare.04577

Numa, A. H., & Newth, C. J. (1996). Anatomic dead space in infants and children. *Journal of applied physiology*, 80(5), 1485–1489. https://doi.org/10.1152/jappl.1996.80.5.1485

Papazian, L., Corley, A., Hess, D., Fraser, J. F., Frat, J. P., Guitton, C., Jaber, S., Maggiore, S. M., Nava, S., Rello, J., Ricard, J. D., Stephan, F., Trisolini, R., & Azoulay, E. (2016). Use of high-flow nasal cannula oxygenation in ICU adults: a narrative review. *Intensive care medicine*, 42(9), 1336–1349. https://doi.org/10.1007/s00134-016-4277-8

Peterson, R., Hassumani, D., Hole, A., Slaven, J., Tori, A., and Abu-Sultaneh, S. (2021). Implementation of a High-Flow Nasal Cannula Management Protocol in the Pediatric ICU. *Resp care*, 66 (4) 591-599; https://doi.org/10.4187/respcare.08284

Pinto, V. & Sharma, S. (2020). Continuous Positive Airway Pressure. *StatPearls Publishing*. https://www.ncbi.nlm.nih.gov/books/NBK482178/

Ramnarayan, P., & Schibler, A. (2017). Glass half empty or half full? The story of high-flow nasal cannula therapy in critically ill children. *Intensive care medicine*, 43(2), 246–249. https://doi.org/10.1007/s00134-016-4663-2

Santschi, M., Gauvin, F., Hatzakis, G., Lacroix, J., & Jouvet, P. (2007). Acceptable respiratory physiologic limits for children during weaning from mechanical ventilation. *Intensive care medicine*, 33(2), 319–325. https://doi.org/10.1007/s00134-006-0414-0

Schmid, F., Olbertz, DM., & Ballmann, M. (2017). The use of high-flow nasal cannula and pediatric intensive care units in Germany – A nationwide survey. *Respiratory Medicine*, 131(210-214). doi: 10.1016/j.rmed.2017.08.027

Sorkness, R. L., Kienert, C., O'Brien, M. J., Fain, S. B., & Jarjour, N. N. (2019). Compressive air trapping in asthma: effects of age, sex, and severity. Journal of applied physiology

(Bethesda, Md. : 1985), 126(5), 1265–1271.

https://doi.org/10.1152/japplphysiol.00924.2018

Spicuzza, L., & Schisano, M. (2020). High-flow nasal cannula oxygen therapy as an emerging

option for respiratory failure: the present and the future. *Therapeutic advances in chronic*

disease, 11, 2040622320920106. https://doi.org/10.1177/2040622320920106

Spoletini, G., Alotaibi, M., Blasi, F., & Hill, N. S. (2015). Heated Humidified High-Flow Nasal

Oxygen in Adults: Mechanisms of Action and Clinical Implications. *Chest*, 148(1), 253–

261. https://doi.org/10.1378/chest.14-2871

Ward J. J. (2013). High-flow oxygen administration by nasal cannula for adult and perinatal

patients. *Respiratory care*, 58(1), 98–122. https://doi.org/10.4187/respcare.01941

APPENDIX A

Protocol

Non-labored Breathing

1. Switch on the power to Hamilton-G5 Ventilator

2. Run manufacturer flow-sensor calibration

3. Program ventilator with selected parameters

   a. Respiratory rate of 20 breaths per minute (bpm)

   b. Tidal volume 170mL

   c. Flow of 20.4 L/min

      i. Produces I:E ratio of 1:2.8

   d. Sinusoidal waveform

   e. FiO_2 0.21

   f. PEEP of 0 cm H_2O

4. Connect ventilator circuit to positive pressure (side A) of test lung

   a. Lung compliance set at 0.1 L/cm H_2O

5. Activate auxiliary pressure port

   a. Connect auxiliary pressure line to front of ventilator

   b. Connect auxiliary pressure line to adaptor placed in negative airway

6. Start ventilator and allow to cycle for 1 minute

7. Start measurement of control with no high flow device at the orifice of the fabricated

   airway

Vapotherm

1. Recalibrate Hamilton-G5 flow sensor

2. Allow to cycle for 1 minute

3. Plug Vapotherm unit into wall outlet

4. Connect Vapotherm unit to oxygen wall outlet and air wall outlet

5. Switch on the power to Vapotherm unit

6. Turn flow to 10 L/min on Vapotherm unit

7. Position Vapotherm cannula with clamp stand so nasal prongs rest inside fabricated

     airway

8. After securing positioning of the nasal prongs, cycle ventilator for 1 minute

9. Begin recording PIP for 20 breaths (1 minute)

10. Recalibrate Hamilton-G5 flow sensor

11. Allow to cycle for 1 minute

12. Turn flow to 15 L/min on Vapotherm unit

13. Begin recording PIP for 20 breaths (1 minute)

14. Recalibrate Hamilton-G5 flow sensor

15. Allow to cycle for 1 minute

16. Turn flow to 20 L/min on Vapotherm unit

17. Begin recording PIP for 20 breaths (1 minute)

                                        Optiflow+

1. Recalibrate Hamilton-G5 flow sensor

2. Allow to cycle for 1 minute

3. Connect Optiflow+ unit to high-flow flow meter via oxygen tube adaptor

4. Turn flow to 10 L/min on high-flow flow meter

5. Position Optiflow+ cannula with clamp stand so nasal prongs rest inside fabricated airway

6. After securing positioning of the nasal prongs, cycle ventilator for 1 minute

7. Begin recording PIP for 20 breaths (1 minute)

8. Recalibrate Hamilton-G5 flow sensor

9. Allow to cycle for 1 minute

10. Turn flow to 15 L/min on high-flow flow meter

11. Begin recording PIP for 20 breaths (1 minute)

12. Recalibrate Hamilton-G5 flow sensor

13. Allow to cycle for 1 minute

14. Turn flow to 20 L/min on high-flow flow meter

15. Begin recording PIP for 20 breaths (1 minute)

<div align="center">Hudson</div>

1. Recalibrate Hamilton-G5 flow sensor

2. Allow to cycle for 1 minute

3. Connect Hudson unit to high-flow flow meter via oxygen tube adaptor

4. Turn flow to 10 L/min on high-flow flow meter

5. Position Hudson cannula with clamp stand so nasal prongs rest inside fabricated airway

6. After securing positioning of the nasal prongs, cycle ventilator for 1 minute

7. Begin recording PIP for 20 breaths (1 minute)

8. Recalibrate Hamilton-G5 flow sensor

9. Allow to cycle for 1 minute

10. Turn flow to 15 L/min on high-flow flow meter

11. Begin recording PIP for 20 breaths (1 minute)

12. Recalibrate Hamilton-G5 flow sensor

13. Allow to cycle for 1 minute

14. Turn flow to 20 L/min on high-flow flow meter

15. Begin recording PIP for 20 breaths (1 minute)

APPENDIX B

Protocol

Labored Breathing

1. Switch on the power to Hamilton-G5 Ventilator

2. Run manufacturer flow-sensor calibration

3. Program ventilator with selected parameters

   a. Respiratory rate of 40 bpm

   b. Tidal volume 170mL

   c. Flow of 40.8 L/min

      i. Produces I:E ratio of 1:2.8

   d. Sinusoidal waveform

   e. FiO_2 0.21

   f. PEEP of 0 cm H_2O

4. Connect ventilator circuit to positive pressure (side A) of test lung

   a. Lung compliance set at 0.1 L/cm H_2O

5. Activate auxiliary pressure port

   a. Connect auxiliary pressure line to front of ventilator

   b. Connect auxiliary pressure line to adaptor placed in negative airway

6. Start ventilator and allow to cycle for 1 minute

7. Start measurement of control with no high flow device at the orifice of the fabricated

   airway

Vapotherm

1. Recalibrate Hamilton-G5 flow sensor

2. Allow to cycle for 1 minute

3. Plug Vapotherm unit into wall outlet

4. Connect Vapotherm unit to oxygen wall outlet and air wall outlet

5. Switch on the power to Vapotherm unit

6. Turn flow to 10 L/min on Vapotherm unit

7. Position Vapotherm cannula with clamp stand so nasal prongs rest inside fabricated

    airway

8. After securing positioning of the nasal prongs, cycle ventilator for 1 minute

9. Begin recording PIP for 20 breaths (1 minute)

     a. Start recording on breath number 2

     b. Record every breath for total of 20 recordings (n=20)

10. Recalibrate Hamilton-G5 flow sensor

11. Allow to cycle for 1 minute

12. Turn flow to 15 L/min on Vapotherm unit

13. Begin recording PIP for 20 breaths (1 minute)

     a. Start recording on breath number 2

     b. Record every breath for total of 20 recordings (n=20)

14. Recalibrate Hamilton-G5 flow sensor

15. Allow to cycle for 1 minute

16. Turn flow to 20 L/min on Vapotherm unit

17. Begin recording PIP for 20 breaths (1 minute)

     a. Start recording on breath number 2

     b. Record every breath for total of 20 recordings (n=20)

Optiflow+

1. Recalibrate Hamilton-G5 flow sensor

2. Allow to cycle for 1 minute

3. Connect Optiflow+ unit to high-flow flow meter via oxygen tube adaptor

4. Turn flow to 10 L/min on high-flow flow meter

5. Position Optiflow+ cannula with clamp stand so nasal prongs rest inside fabricated

    airway

6. After securing positioning of the nasal prongs, cycle ventilator for 1 minute

7. Begin recording PIP for 20 breaths (1 minute)

    a. Start recording on breath number 2

    b. Record every breath for total of 20 recordings (n=20)

8. Recalibrate Hamilton-G5 flow sensor

9. Allow to cycle for 1 minute

10. Turn flow to 15 L/min on high-flow flow meter

11. Begin recording PIP for 20 breaths (1 minute)

    a. Start recording on breath number 2

    b. Record every breath for total of 20 recordings (n=20)

12. Recalibrate Hamilton-G5 flow sensor

13. Allow to cycle for 1 minute

14. Turn flow to 20 L/min on high-flow flow meter

15. Begin recording PIP for 20 breaths (1 minute)

    a. Start recording on breath number 2

    b. Record every breath for total of 20 recordings (n=20)

Hudson

1. Recalibrate Hamilton-G5 flow sensor

2. Allow to cycle for 1 minute

3. Connect Hudson unit to high-flow flow meter via oxygen tube adaptor

4. Turn flow to 10 L/min on high-flow flow meter

5. Position Hudson cannula with clamp stand so nasal prongs rest inside fabricated airway

6. After securing positioning of the nasal prongs, cycle ventilator for 1 minute

7. Begin recording PIP for 20 breaths (1 minute)

   a. Start recording on breath number 2

   b. Record every breath for total of 20 recordings (n=20)

8. Recalibrate Hamilton-G5 flow sensor

9. Allow to cycle for 1 minute

10. Turn flow to 15 L/min on high-flow flow meter

11. Begin recording PIP for 20 breaths (1 minute)

    a. Start recording on breath number 2

    b. Record every breath for total of 20 recordings (n=20)

12. Recalibrate Hamilton-G5 flow sensor

13. Allow to cycle for 1 minute

14. Turn flow to 20 L/min on high-flow flow meter

15. Begin recording PIP for 20 breaths (1 minute)

    a. Start recording on breath number 2

    b. Record every breath for total of 20 recordings (n=20)